Supplementary Information for

"Influences of lone-pair electrons on directionality of hydrogen bonds formed by hydrophilic amino acids in molecular dynamics simulation"

Tomotaka Oroguchi [a,b,*] and Masayoshi Nakasako [a,b]

[a]Department of Physics, Faculty of Science and Technology, Keio University,

3-14-1 Hiyoshi, Kohoku-ku, Yokohama, 223-8522 Japan

[b]RIKEN SPring-8 Center, 1-1-1 Kohto, Sayo, Sayo-gun, Hyogo 679-5148 Japan

[*] To whom correspondence should be addressed. Phone: +81-45-566-1703. Fax: +81-45-566-1672.

E-mail: oroguchi@phys.keio.ac.jp.

Supplementary Note 1: Convergence of hydration structure

The width of the time-window, in which the solvent density maps calculated from a MD trajectory, was first investigated for a 10-ns production run of both the MD-LP and MD-noLP simulations for the Gly-Glu-Lys-Gly (GEKG) peptide. Supplementary Figure S1 compares the solvent density maps of oxygen atoms in hydration water molecules around the peptide calculated for the time-windows of 1.0-1.2, 1.0-1.5 and 1.0-3.0 ns in the production run with that calculated from the EHDF. The map from the time-window of 1.0-1.2 ns displayed noise in the bulk region, indicating the insufficient window width. In the map of the time-window of 1.0-1.5 ns, the noise level was significantly reduced. The time-window of 1.0-3.0 ns gave the solvent density map with the noise densities at very small levels. The map was suitable to compare with that from the EHDF. Supplementary Figure S2 shows the solvent density maps of oxygen and hydrogen atoms of hydration water molecules around the OE1 and OE2 atoms calculated for the time-windows of 1.0-1.2, 1.0-1.5, 1.0-2.0 and 1.0-3.0 ns. As well as the maps in Figure S1, wider time-window gave maps with lower noise levels both in the density maps and in the profiles of distance and angular distributions. These tendencies were common between the MD-LP and MD-noLP simulations. Therefore, we set the size of the time-window at 1 ns in this study.

Next, we examined whether the solvent densities calculated by using the 1-ns time-window gave almost the same maps at any moment in the 10-ns trajectory. Supplementary Figure S3 compares the solvent density maps calculated in the time-intervals of 1-2, 4-5 and 9-10 ns in the trajectory. The maps were almost independent of the three calculations. Around the OE1 and OE2 atoms of glutamate side chain, the solvent density distributions calculated in the time-intervals of 1-2, 4-5 and 9-10 ns were also equivalent with each other (Supplementary Fig. S4). This tendency was common in both the MD-LP and MD-noLP simulations. Therefore, these results allowed us to calculate the solvent density distributions for the last 1 ns in a 2-ns production run of peptides for comparisons with the EHDFs.

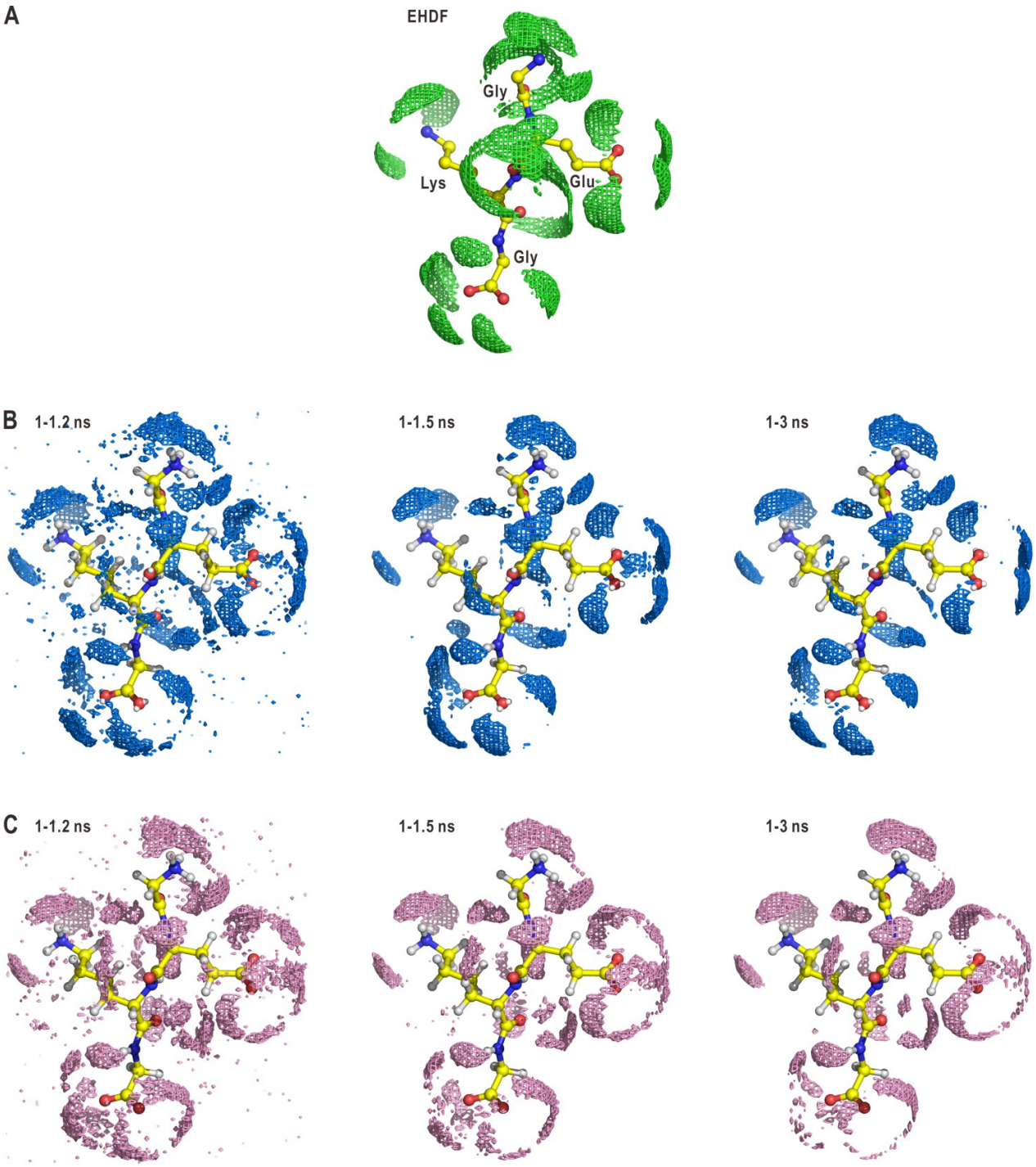

Supplementary Figure S1. (A) Solvent density map of oxygen atoms in hydration water molecules around the GEKG peptide predicted by using the EHDFs. Solvent density maps obtained from the 1-1.2,

1-1.5, and 1-3 ns trajectories of the MD-LP (B) and MD-noLP (C) simulations of 10 ns. The density maps are contoured at 1.6 e·Å^{-3}.

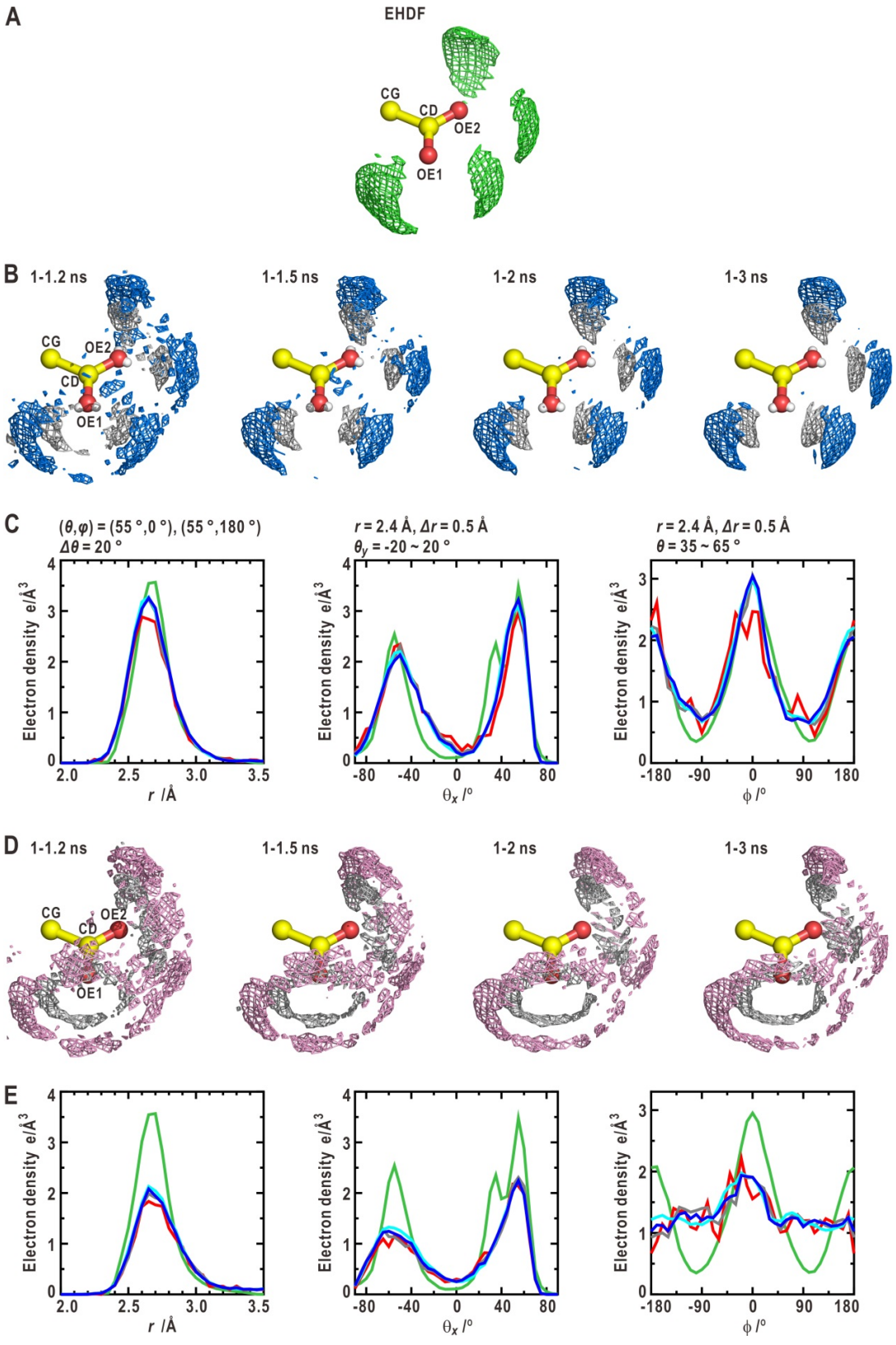
A
EHDF
CG
CD
OE2
OE1
B
1-1.2 ns
1-1.5 ns
1-2 ns
1-3 ns
C
(θ,φ) = (55 °,0 °), (55 °,180 °)
Δθ = 20 °
r = 2.4 Å, Δr = 0.5 Å
θy = -20 ~ 20 °
r = 2.4 Å, Δr = 0.5 Å
θ = 35 ~ 65 °
Electron density e/Å3
r /Å
θx /°
ϕ /°
D
1-1.2 ns
1-1.5 ns
1-2 ns
1-3 ns
E
Electron density e/Å3
r /Å
θx /°
ϕ /°

Supplementary Figure S2. (A) Solvent density maps, which display the distribution of oxygen and/or hydrogen atoms in hydration water molecules, around the OE1 and OE2 atoms in the side chain of glutamate in the GEKG peptide predicted by using the EHDFs. (B) Solvent density maps calculated from the 1-1.2, 1-1.5, 1-2, and 1-3 ns trajectories of the 10-ns MD-LP simulation. The positions of the LP charge sites used in the MD-LP simulation are indicated by the small white spheres. The density maps for oxygen atoms in the EHDF (green), MD-LP (blue) and MD-noLP (pink) simulations, and for hydrogen atoms (white) are contoured at 1.6 and 0.4 $e \cdot Å^{-3}$, respectively. These schemes are used in the subsequent illustrations of solvent density maps in the Supplementary Information. (C) The profiles of distance (left), θ_x (center) and φ (right) distributions of oxygen atoms in hydration water molecules in the MD-LP simulation. The distance distribution is calculated by averaging those in the four clusters of the solvent densities. In addition, the two angular distributions are averaged for the solvent densities around the OE1 and OE2 atoms. The parameters necessary for these calculations in the coordinate system shown in Fig. 1B of the main text are labelled at the top of each plot. The scheme for plotting the profiles is also used in the subsequent illustrations in the Supplementary Information. Profile of the EHDF (green) is compared with those calculated from the 1.0-1.2 (red), 1.0-1.5 (grey), 1.0-2.0 (blue), and 1.0-3.0 (cyan) ns trajectories. Solvent density maps (D) and distribution profiles (E) calculated from the 1-1.2, 1-1.5, 1-2, and 1-3 ns trajectories of the 10-ns MD-noLP simulation.

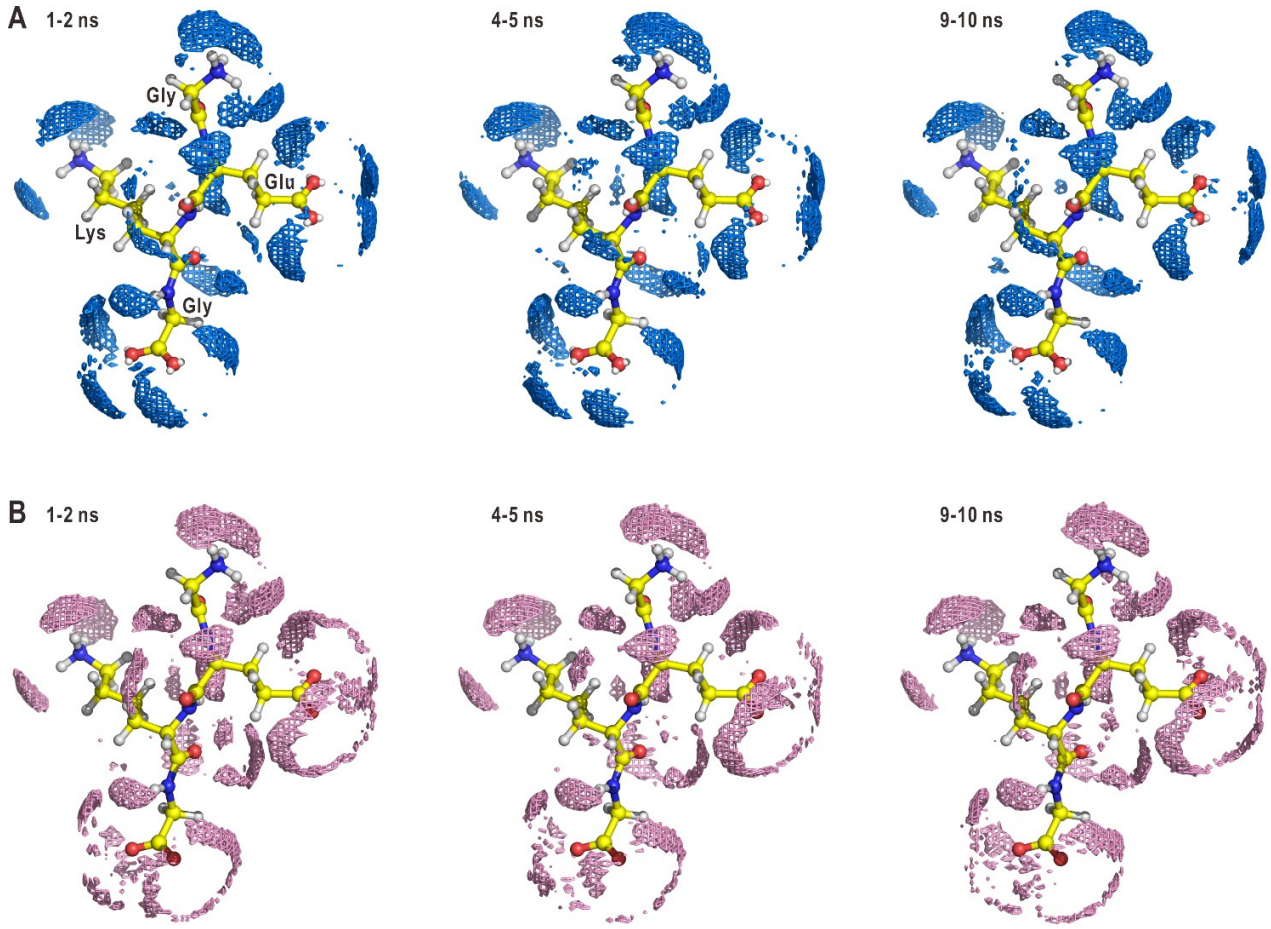

Supplementary Figure S3. Solvent density maps of oxygen atoms in hydration water molecules around the GEKG peptide obtained from the 1-2, 4-5, and 9-10 ns trajectories of the MD-LP (A) and MD-noLP (B) simulations of 10 ns.

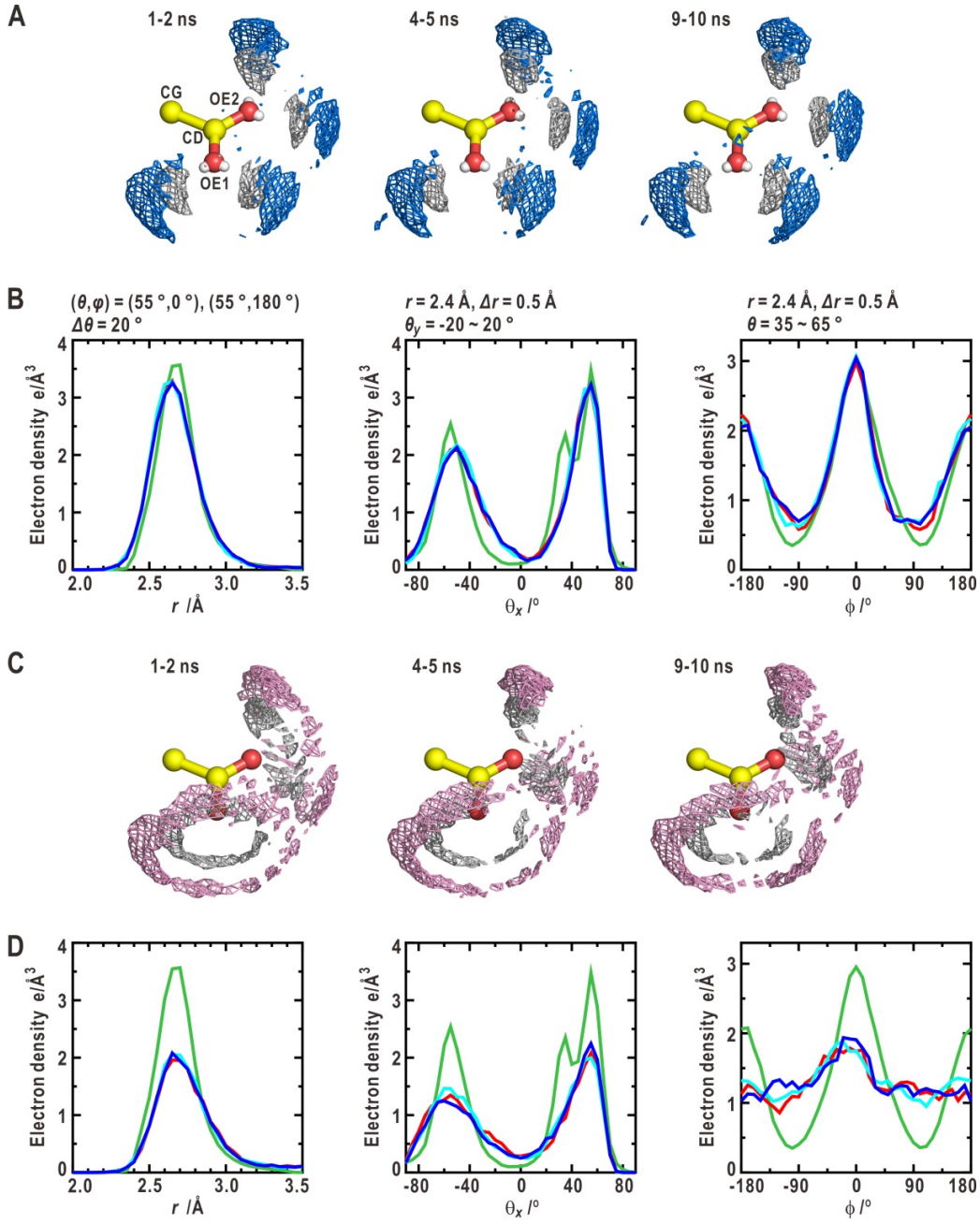

Supplementary Figure S4. Solvent density maps and the distribution profiles around the OE1 and OE2 atoms in the side chain of glutamate calculated from the 1-2, 4-5 and 9-10 ns time-intervals for the 10-ns MD-LP (panels (A) and (B)) and MD-noLP (panels (C) and (D)) simulations. The distance (left), θ_x (center), and φ (right) distributions of oxygen atoms in hydration water molecules were averaged around the OE1 and OE2 atoms. The profile of the EHDF (green) are compared with those from the 1-2 (blue),

4-5 (red) and 9-10 (cyan) ns intervals.

Supplementary Note 2: Hydration structures around the deprotonated sp^2-hybridized oxygen atoms in aspartate

Supplementary Figure S5 shows the solvent density distribution around the deprotonated sp^2-hybridized OD1 and OD2 atoms in the side chain of the aspartate. The MD-LP simulation reproduced the distribution of oxygen atoms of hydration water molecules in the EHDF regarding the profiles and peak positions in the distance and angular distributions (Supplementary Fig. S5C and Table 1). The simulation gave four density peaks of the oxygen atoms of the hydration water molecules. The center of each of these peaks was located in the directions of OD1(OD2)-LP ((θ_x, φ) = (+55°, 0°) and (−55°, 180°)). The density peak of the hydrogen atoms of water molecules appeared between the OD1 (OD2) atom and the density peak of water oxygen atoms, indicating the directionality of the H-bond.

The MD-noLP simulation gave a solvent density distribution different from that of the MD-LP simulation and the EHDF. The oxygen atoms of the hydration water molecules around the OD1 (OD2) atom were distributed in toroidal shape, the center of which was located in the CG-OD1 (CG-OD2) direction, and had little prominent peaks in the φ distribution (Supplementary Fig. S5C and Table 1). The densities of the hydration water molecules residing around the OD1 (OD2) atom were smaller than those in the MD-LP simulation, suggesting that the interaction between OD1 (OD2) and hydration water molecules is weaker than that in the MD-LP simulation. Between the oxygen atoms of the hydration water molecules and OD1 (OD2) atoms, the hydrogen atoms of the hydration water molecules were distributed in an arc shape.

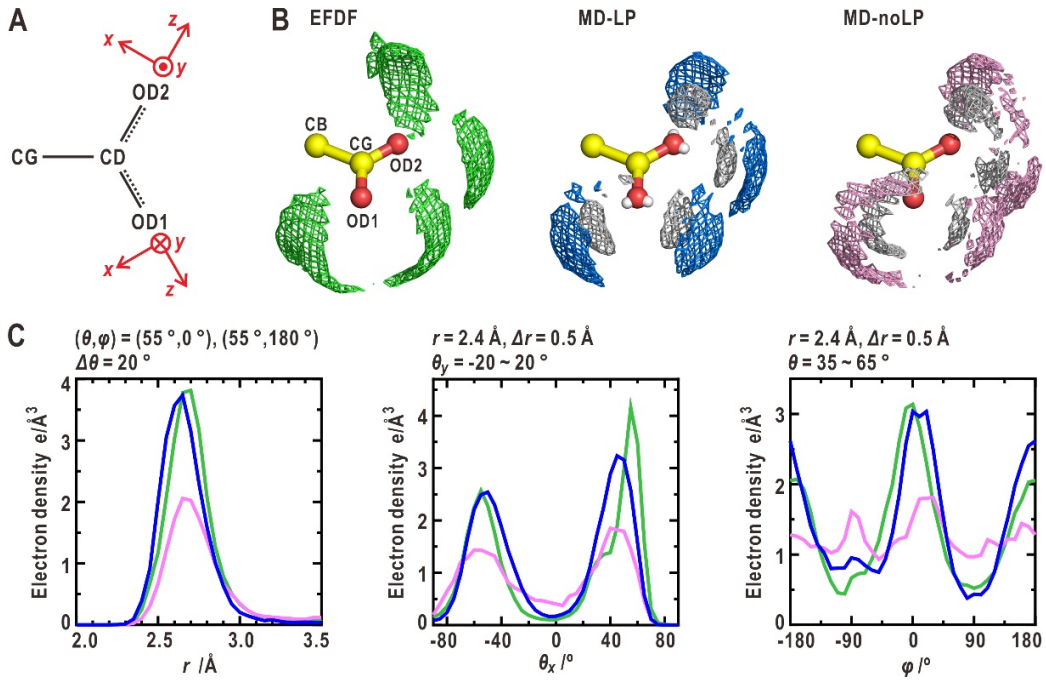

Supplementary Figure S5. (A) The coordinate systems used for describing the solvent density distribution around the OD1 and OD2 atoms in the side chain of aspartate. (B) Comparison of the solvent density maps around the OD1 and OD2 atoms among the EHDF, and MD-LP and MD-noLP simulations for the Gly-Asp-Lys-Gly (GDKG) peptide. (C) The profiles of the distance (left panel), θ_x (center), and φ (right) distributions of oxygen atoms in hydration water molecules. The distance distribution is calculated by averaging the four clusters of the solvent densities of the oxygen atoms. The θ_x- and φ-distributions are averaged over the solvent densities around the OD1 and OD2 atoms. The green, blue, and pink lines are the profiles from the EHDF, MD-LP, and MD-noLP simulations, respectively. The coloring for plotting the profiles is also used in the subsequent illustrations in the Supplementary Information.

Supplementary Note 3: Hydration structure around the side chain of histidine in the HID state

Around the protonated ND1 atom, the MD-LP and MD-noLP simulations gave the distribution of oxygen atoms of hydration water molecules similar to that of the EHDF with respect to the peak positions and profiles in the angular (θ_x and θ_y) distributions (Supplementary Fig. S6 and Table 1). However, the densities of the hydration water molecules residing around the ND1 atom were smaller than those in the EHDF (Supplementary Fig. S6C). The peak positions and profiles of the distance distributions in the simulations were inconsistent with those in the EHDF. For simulating better the EHDF regarding the profiles in the distance and angular distributions, more attractive interactions between the hydration water molecules and the N-H group would be necessary

Regarding the deprotonated sp^2-hybridized NE2 atom, the MD-LP simulation simulated well the angular distribution in the EHDF (Supplementary Fig. S6D). In contrast, the distance distribution of the solvent density differed from that of the EHDF regarding the peak position (2.65 Å in the MD-LP, and 2.75 Å in the EHDF) and the profile. When the NE2-LP charge pair has less attractive interactions with hydration water molecules in the simulation, the differences would become small. In the MD-noLP simulation, the hydration water molecules around the NE2 atom were distributed in a wide range of θ_y with two broad maxima at $\theta_y = \pm 80°$, while the θ_y-distribution of the EHDF and the MD-LP simulation had single peaks at $\theta_y = 0°$. This finding suggests that the LP set at the NE2 atom in the MD-LP simulation is necessary to localize the hydration water molecules within the plane of the imidazole ring.

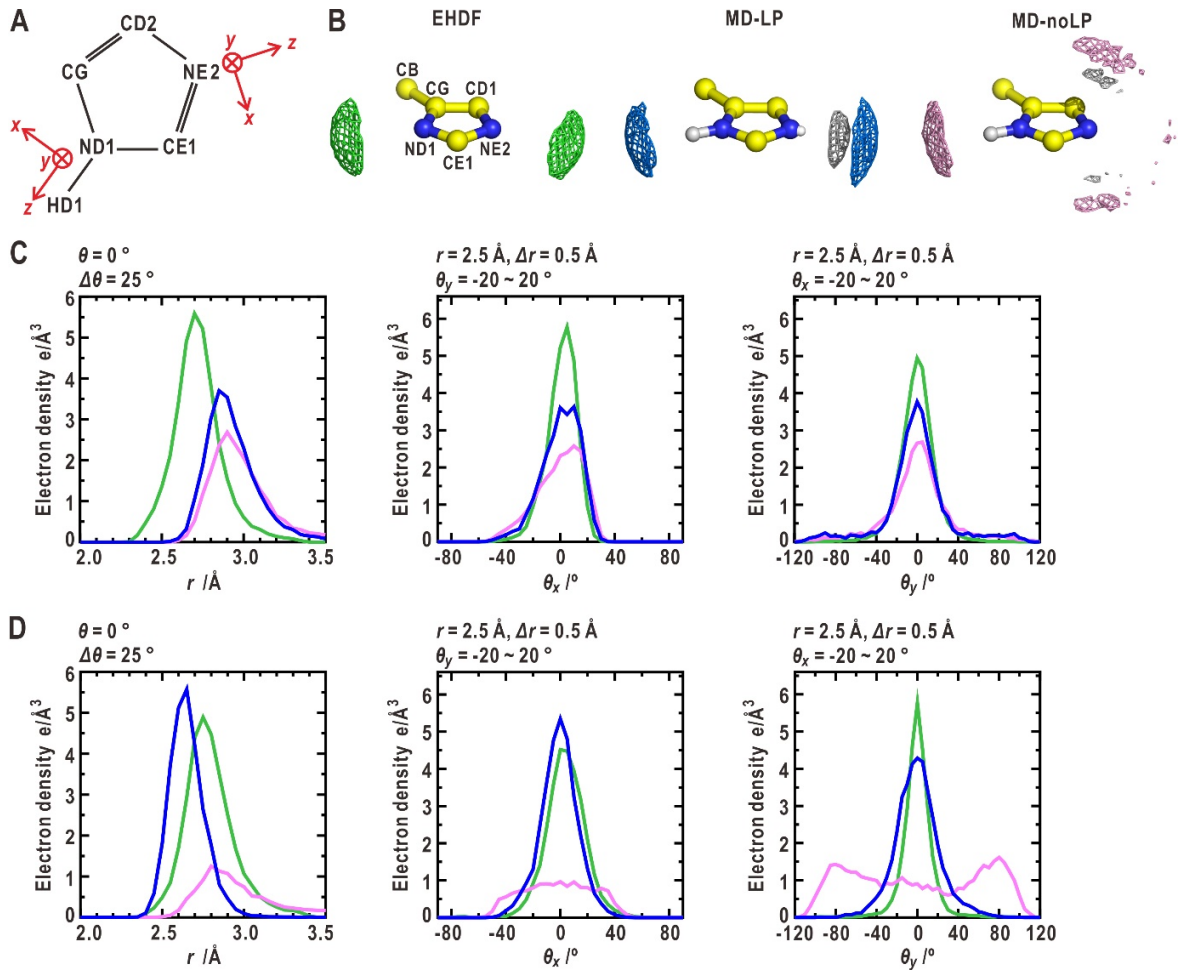

Supplementary Figure S6. (A) The coordinate systems used for describing the solvent density distributions around the ND1 and NE2 atoms in the imidazole ring of histidine. (B) Comparison of the solvent density maps around the imidazole ring of histidine among the EHDF, and MD-LP and MD-noLP simulations for the Gly-His (HID state)-Gly tripeptide. The profiles of distance (left panel), θ_x (center), and θ_y (right) distributions of the water oxygen densities around the ND1 and NE1 atoms are plotted in panels (C) and (D), respectively.

Supplementary Note 4: Hydration structures around the protonated oxygen atoms in the *sp*^{3}-hybridization in the side chains of serine and threonine

In the EHDFs around the OG atom of serine (Supplementary Fig. S7B) and the OG1 atom of threonine (Supplementary Fig. S8B), the solvent densities are distributed in semi-toroidal shapes with three prominent peaks at $\varphi = 0°$ and ±90°. These peaks are attributed to the three configurations of the CB-OG (CB-OG1) bond (Supplementary Figs. S7C-E and S8C-E). Therefore, MD simulations were conducted for the three configurations. The solvent densities were summed over the simulations and normalized so that the total sum of the densities within the toroid was equal to that in the EHDFs. In the MD-LP simulation, two LPs on the side opposite to the OG-HG (OG1-HG1) bond were modeled by assuming that the OG (OG1) atom of serine (threonine) is in the *sp*^{3}-hybridization.

The MD-LP and MD-noLP simulations for each configuration gave almost the same solvent density distributions both around serine (Supplementary Fig. S7C-E) and threonine (Supplementary Fig. S8C-E). They were composed of two major peaks with narrow widths and another with a broad maximum (Table 1). For the configuration in which the dihedral angle of CA-CB-OG(OG1)-HG(HG1) was 0°, a major peak appeared in the direction of $\varphi = 0°$. A broad minor peak in the opposite direction of the major peak ($-180° < \varphi < -90°$, $90° < \varphi < 180°$) was caused by the frequent residence of the hydration water molecules in a narrow pocket formed between the side and main chains. Since the peak was absent from the EHDFs and independent of the two MD simulations, the van der Waals attractions between the hydration water molecules and the atoms forming the pocket were predominant, rather than the dipole-dipole interactions between the hydration water molecules and the OG(OG1)-LPs.

For the configuration, in which the dihedral angle was ±90°, the major density peak appeared at $\varphi =$ ±90°, identical to those found in the EHDFs of serine and threonine. The minor peak located on the opposite side of the OG-HG (OG1-HG1) bond was smaller than that observed in the case where the dihedral angle was 0°. The hydration water molecules comprising the minor peaks had contacts with the

atoms forming the main chain. Consequently, the dipole-dipole interactions with the OG-LPs would have little influence on their residence in the region of the minor peaks, because the shape and size of the minor peaks were independent of the MD-LP and MD-noLP simulations.

In both serine and threonine, the summed solvent densities resembled that of the EHDFs with respect to the profiles including the peak positions, except for the influences from the minor peaks (Supplementary Figs. S7F-G and S8F-G, and Table 1). It is also noteworthy that the minor differences in the distributions from the MD-LP and MD-noLP simulations was consistent with the present results for tyrosine (Fig. 4) and also with the other theoretical studies using QM calculations[1,2]. These results and the analysis for the tyrosine side chain indicate that the LP electrons exert a minor influence on the hydration structures around the protonated sp^3-hybridized oxygen atoms.

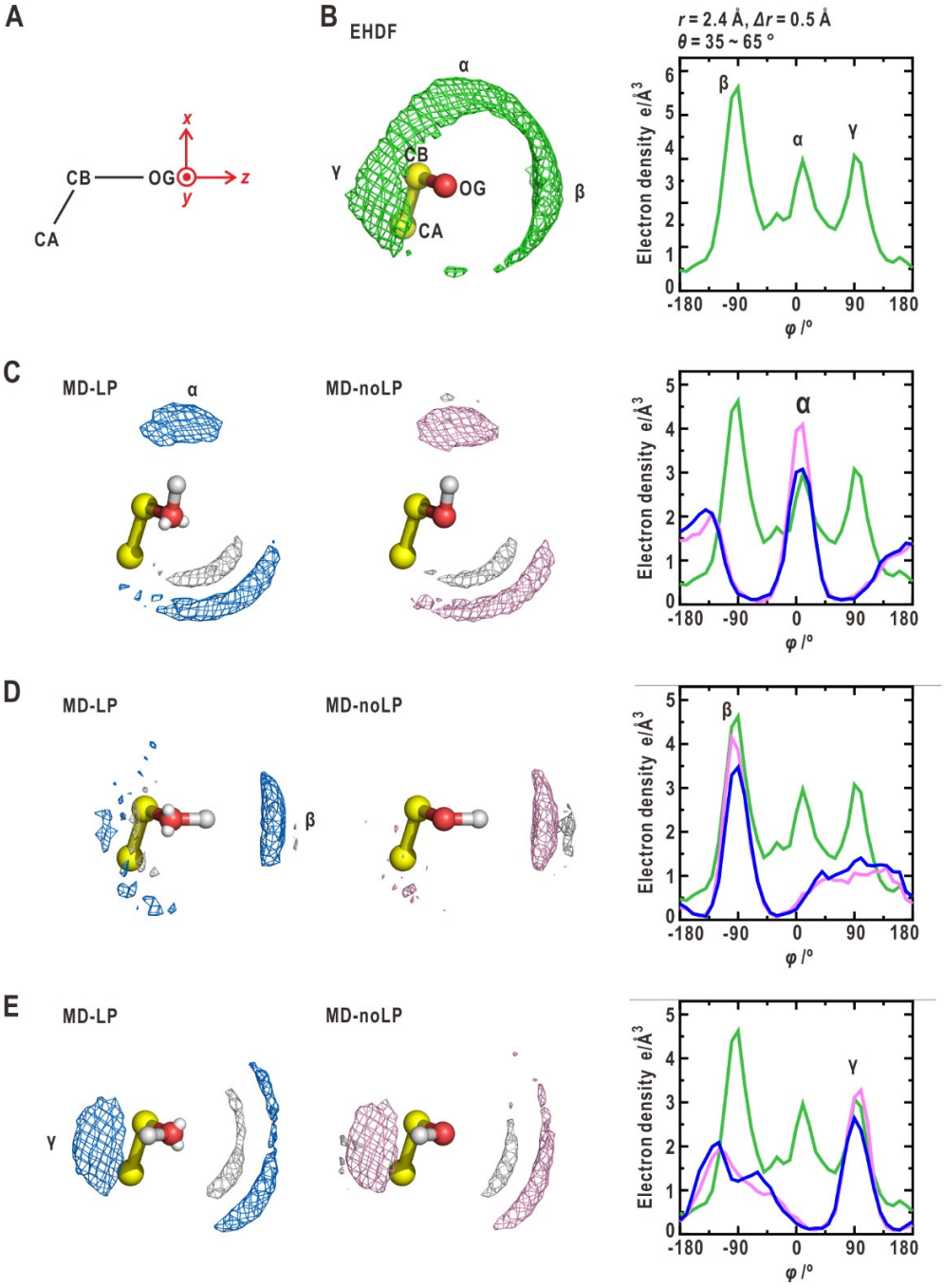
A
CB
OG
CA
x
y
z
B
EHDF
α
γ
β
CB
OG
CA
r = 2.4 Å, Δr = 0.5 Å
θ = 35 ~ 65 °
Electron density e/Å3
φ /°
C
MD-LP
MD-noLP
α
D
MD-LP
MD-noLP
β
E
MD-LP
MD-noLP
γ

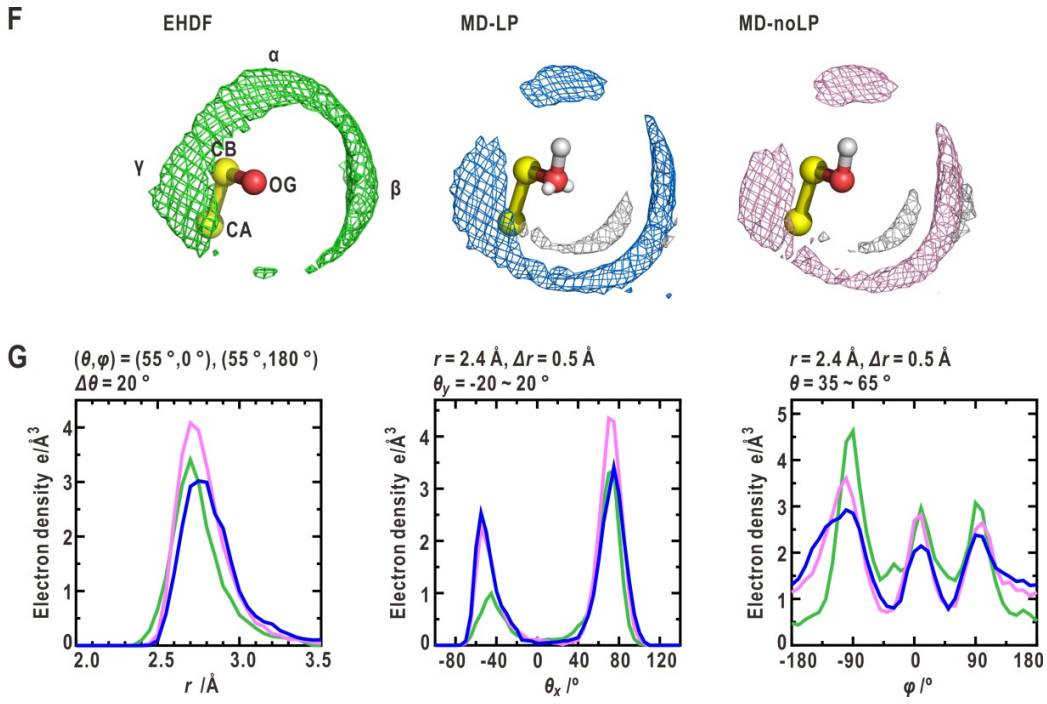

Supplementary Figure S7. (A) The coordinate system used for describing the solvent density distributions around the OG atom in the side chain of serine. (B) The solvent density map around the OG atom in the EHDF (left panel), and the φ distribution (right). The three prominent peaks in the φ distribution are labeled as α, β, and γ. The solvent density distributions in the configurations of CA-CB-OG-HG at the torsion angles of –180° (C), –90° (D), and +90° (E) are compared between the MD-LP and MD-noLP simulations. The profiles of φ-distributions of oxygen atoms in hydration water molecules in the MD-LP (blue line) and MD-noLP (pink) simulations are plotted and compared with that of the EHDF (green) in the right panels. (F) Comparison of the solvent density map of the EHDF with those of oxygen atoms in hydration water molecules summed over the three configurations in the MD-LP and MD-noLP simulations. (G) The profiles of distance (left), θ_x (center), and φ (right) distributions of solvent densities of the EHDF, summed densities of oxygen atoms in hydration water molecules in the MD-LP and MD-noLP simulations.

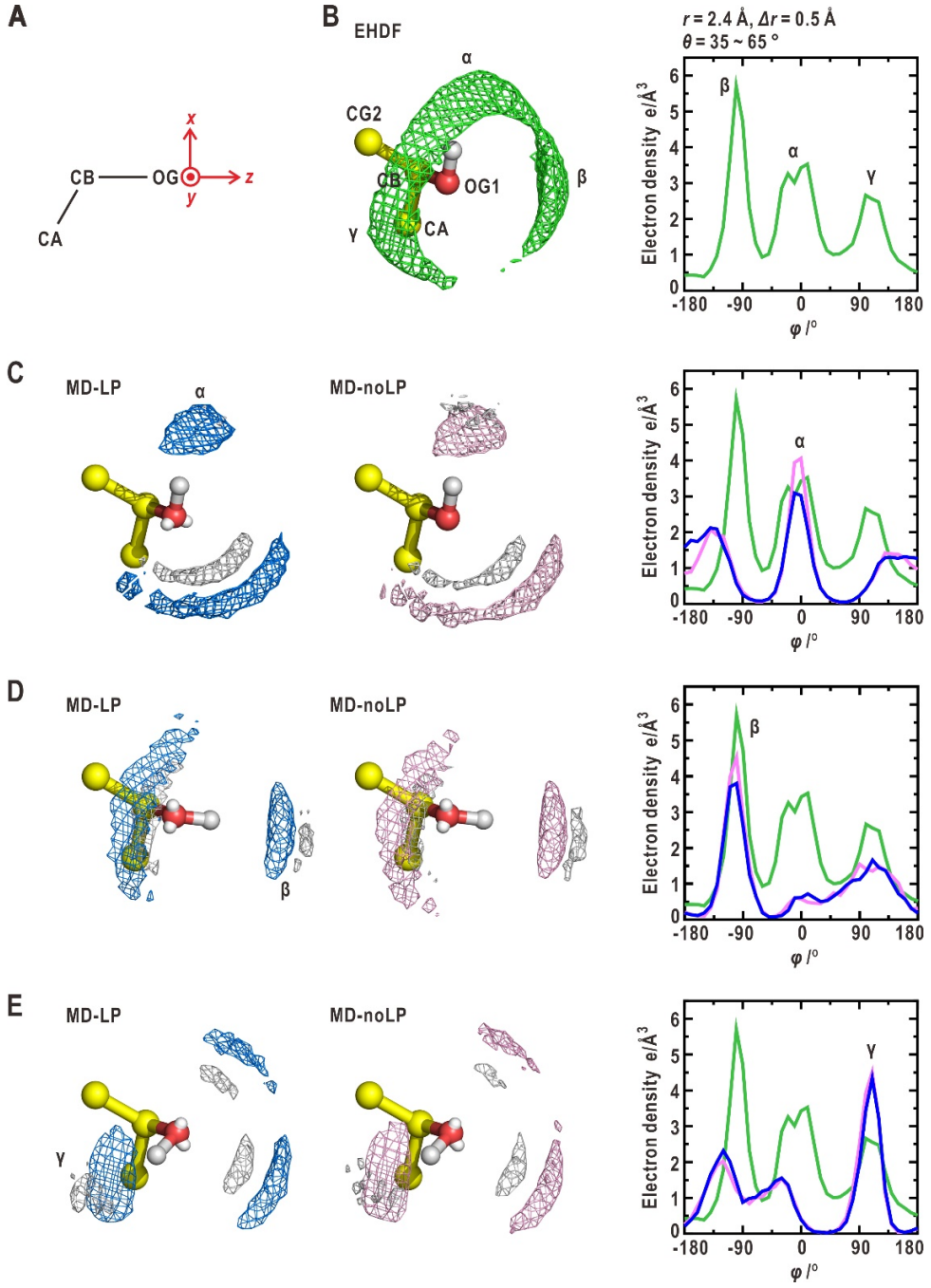
A
CB
OG
CA
x
y
z
B
EHDF
α
CG2
CB
OG1
β
γ
CA
r = 2.4 Å, Δr = 0.5 Å
θ = 35 ~ 65 °
Electron density e/Å3
φ /°
C
MD-LP
MD-noLP
D
MD-LP
MD-noLP
E
MD-LP
MD-noLP

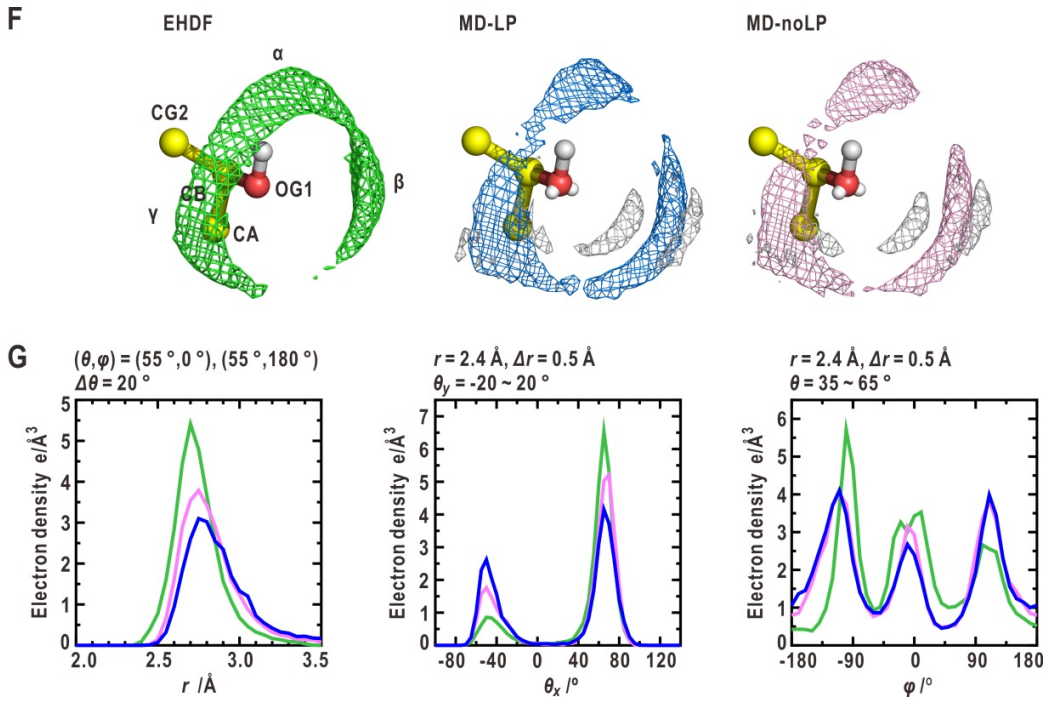

Supplementary Figure S8. (A) The coordinate system used for describing the solvent density distributions around the OG1 atom in the side chain of threonine. (B) The solvent density map around the OG1 atom in the EHDF (left panel), and the φ distribution (right). The three prominent peaks in the φ distribution are labeled as α, β, and γ. The solvent density distributions in the configurations of CA-CB-OG1-HG1 at the torsion angles of –180° (C), –90° (D), and +90° (E) are compared between the MD-LP and MD-noLP simulations. The profiles of φ-distributions of oxygen atoms in hydration water molecules in the MD-LP (blue line) and MD-noLP (pink) simulations are plotted and compared with that of the EHDF (green) in the right panels. (F) Comparison of the solvent density map of the EHDF with those of oxygen atoms in hydration water molecules summed over the three configurations in the MD-LP and MD-noLP simulations. (G) The profiles of distance (left), θ_x (center), and φ (right) distributions of solvent densities of the EHDF, summed densities of oxygen atoms in hydration water molecules in the MD-LP and MD-noLP simulations.

Supplementary Note 5: Hydration structure around the protonated oxygen atom in the *sp*^{2}-hybridization in the side chain of tyrosine

The OH atom in the side chain of tyrosine is typically assumed to be *sp*^{3}-hybridized. However, this atom sometimes appears to be *sp*^{2}-hybridized in the crystal structures of proteins[3,4]. Therefore, in this study, the hydration structure around the OH atom in the *sp*^{2}-hybridization was also calculated with the LP charge site determined as described in the Method section of the main text.

The LP charge site of the OH atom was placed on the opposite side of the HH atom. In both the MD-LP and MD-noLP simulations, the solvent densities predominantly appeared in the direction of the OH-HH bond (Supplementary Fig. S9). The density maps resembled those observed in the simulations for the *sp*^{3}-hybridized OH atom with respect to the distance and angular distributions (Supplementary Figs. S9C-D and Table 1).

On the OH-LP side, a single density peak of oxygen atoms in water molecules appeared in the MD-LP simulation. While this density peak resembled those existing on the OH-HH side in terms of the profiles and the peak positions in the distribution (Table 1), the densities of the hydration water molecules forming the density peaks were smaller than those of the OH-HH side (Supplementary Figs. S9D-E). The hydrogen atoms of hydration water molecules were localized between the oxygen atoms of water molecules and the OH atom of tyrosine, indicating the directionality of the H-bond. The peak position in the distance distribution suggests that the interactions between the hydration water molecules and the OH-LP group are quite weak.

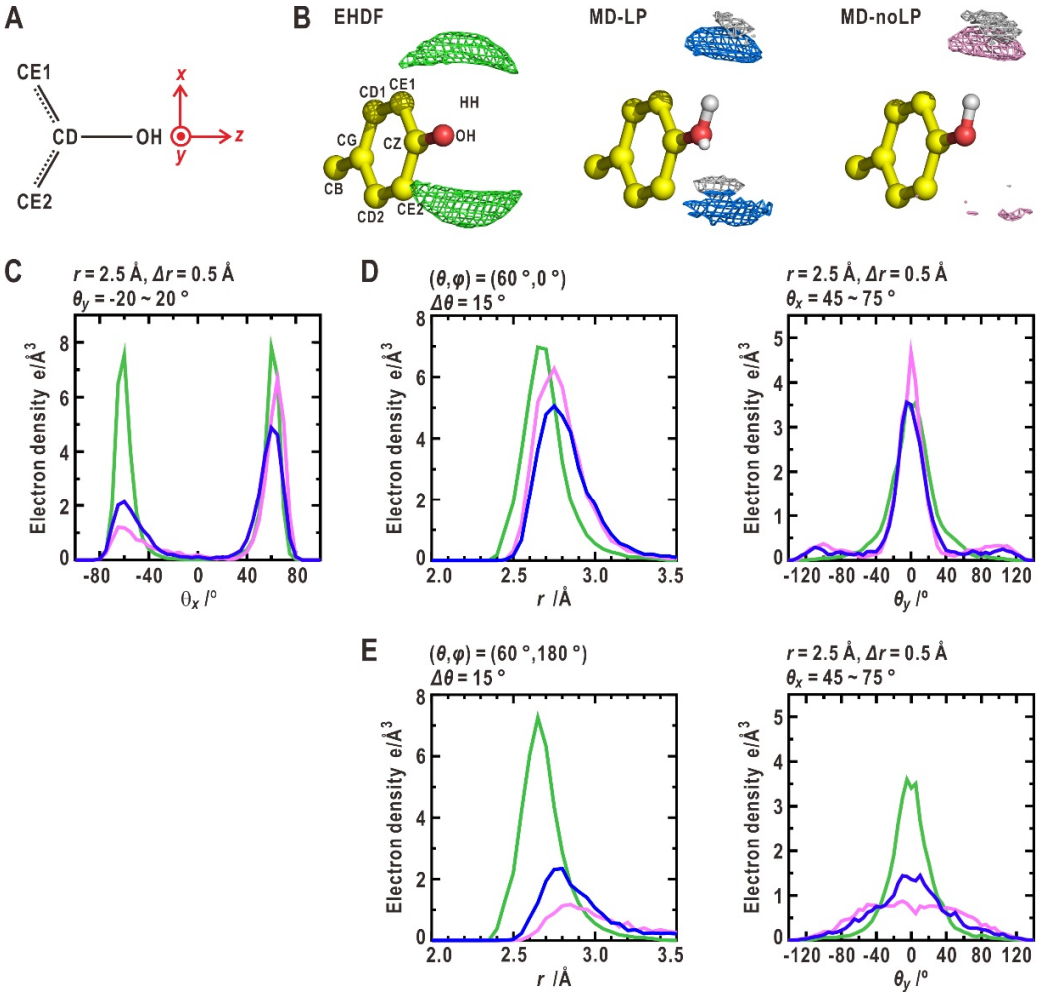

Supplementary Figure S9. (A) The coordinate system used for describing the solvent density distributions around the OH atom in the side chain of tyrosine. (B) Comparison of the solvent density maps around the sp^2-hybridized OH atom among the EHDF, MD-LP and MD-noLP simulations. (C) The θ_x distribution of water oxygen densities around the protonated OH atom. The distance and θ_y distributions on the (D) OH-HH bond side of the protonated OH atom and (E) OH-LP side.

Supplementary Note 6: Hydration structure around the protonated nitrogen atom of the side chain of tryptophan

The NE1 atom in the side chain of tryptophan is protonated under physiological conditions. Both the MD-LP and MD-noLP simulations reproduced the hydration structures observed in the EHDF (Supplementary Fig. S10) of tryptophan, as well as the case for lysine, and arginine. In all these hydration structures, the single density peak of water oxygen atoms appeared in the direction of the NE1-HE1 bond ($\theta_x = \theta_y = 0°$ in the θ_x and θ_y distributions). However, the N atom was less hydrated in these simulations compared to that found in the EHDF (Table 1). One likely reason for this difference might be the small polarization of the NE1-HE1 group determined by the RESP procedure and under the normalization condition of the EHDF, in which one water molecule is supposed to form a hydrogen bond with this group. These points should be addressed in future studies.

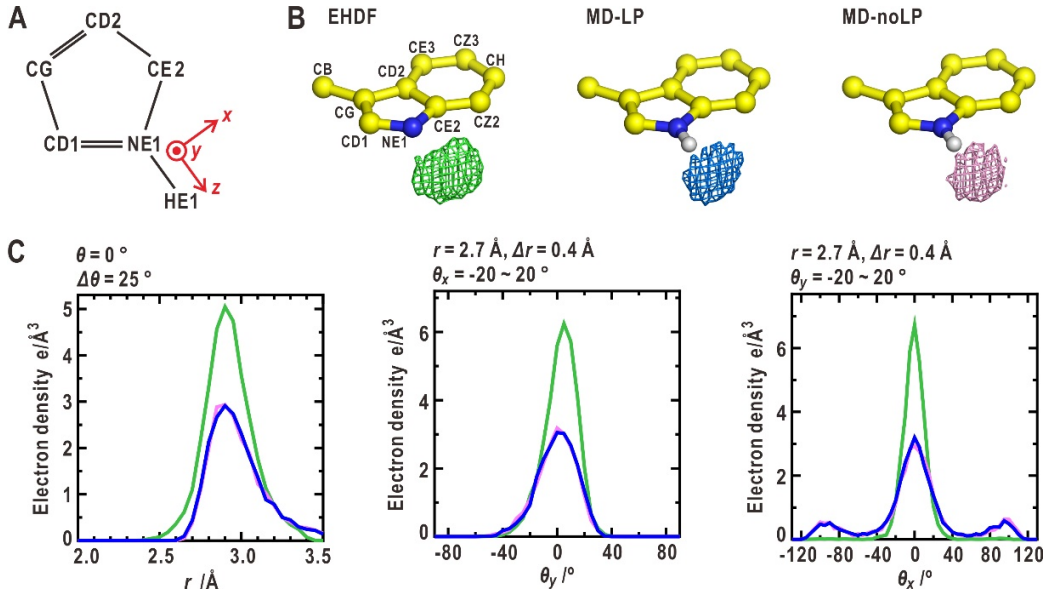

Supplementary Figure S10. (A) The coordinate system used for describing the solvent density distributions around the NE1 atom in the side chain of tryptophan. (B) Comparison of the solvent density maps around the NE1 atom among the EHDF, and MD-LP and MD-noLP simulations. (C) The profiles of distance (left panel), θ_x (center), and θ_y (right) distributions of water oxygen densities around the protonated NE1 atom.

Supplementary Note 7: EHDF for glutamine and asparagine

The hydration structures around the side chains of glutamine and asparagine, which include both deprotonated sp^2-hybridized oxygen atoms and protonated nitrogen atoms, have not been studied in this work. As reported previously[7], the tips of the side chains in a number of glutamine and asparagine residues in the crystal structures are incorrectly modeled with incorrect torsion angles, even though the structures are refined at resolutions better than 2.2 Å.

The EHDFs for the side chains of these two amino acids are unsuitable for use as references for the MD simulations, and therefore the validation on the geometrical characteristics in the H-bonds formed by the side chains of asparagine and glutamine was difficult at the present time. However, the incorporation of LP charge sites into a force field was possible. The tentatively determined charge values on the protonated nitrogen atom and deprotonated oxygen atom both in their sp^2-hybridization were listed in Table 1.

Supplementary Note 8: Comparison of the solvent density distributions from the MD simulations using the charge sets determined by the present and the standard RESP procedures

By using the standard RESP procedure[6,7], we also determined the charges for glutamate and lysine In the first step, the two structures with the conformations of α-helix and β-strand were constructed for a dipeptide, in which each amino acid was blocked by the acetyl and *N*-methyl groups. The rotamer states of the side chain in each conformation were set to the parameters reported by the literature[7]. Subsequently, the QM-ESPs calculated for those conformations were used to determine the charges of the targeted amino acid by using the multi-conformational RESP fitting with the restraint scheme described in the main text. As well as our RESP procedure applied for the GEKG peptide, the charges were determined for both of the models with and without LP sites. The resultant charge sets were implemented in the AMBER force field, and then the hydration structures around the GEKG peptide were calculated by conducting MD-LP and md-noLP simulations for 2 ns.

The charges on the side chains of glutamine and lysine determined using the present and standard RESP procedures were nearly the same (Supplementary Figs. S11-S13 and Table S4). In both MD-LP and MD-noLP simulations, the solvent density distributions around these side chains were almost the same between the two RESP procedures (Supplementary Figs. S12 and S13). Although two RESP procedures resulted in different charges values on the peptide bonds (Supplementary Table S4), the hydration structures around the main chain were similar (Supplementary Fig. S11). Based on the results described above, we decided to employ the present RESP procedure for the determination of charges in the tri- or tetrapeptides.

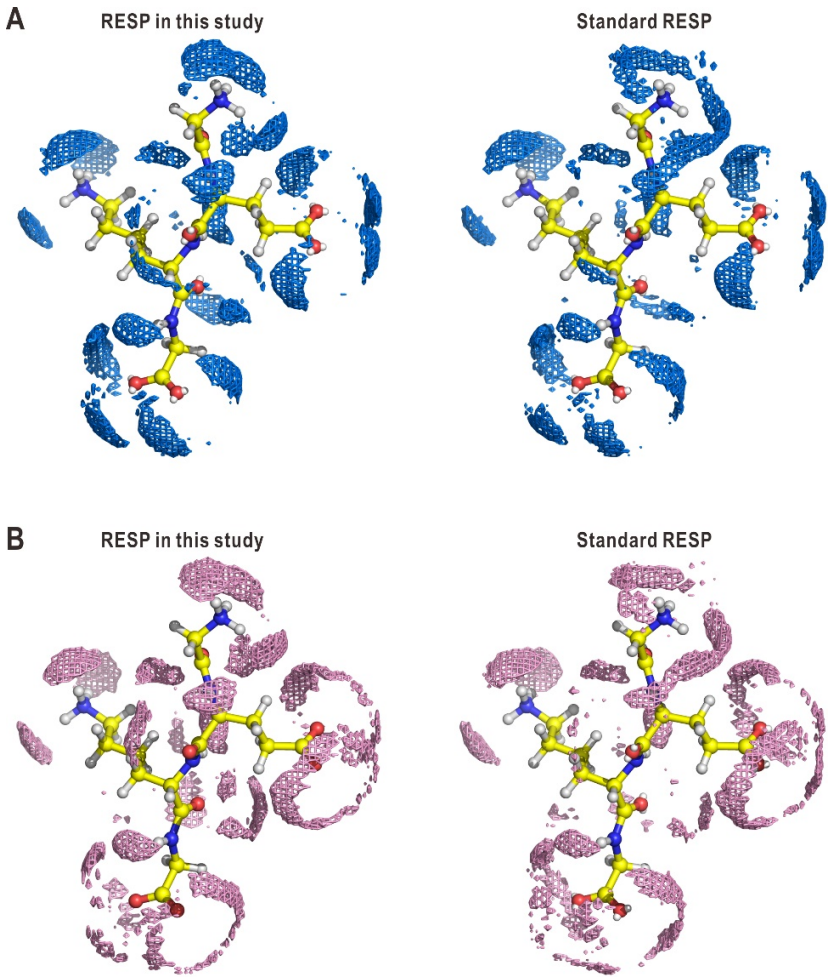

Supplementary Figure S11. (A) Solvent density maps of oxygen atoms in hydration water molecules around the GEKG peptide from the MD-LP simulations using the charges determined by the present (left) and the standard (right) RESP procedures. (B) Solvent density maps from the MD-noLP simulations using the charges determined by the present (left) and the standard (right) RESP procedures.

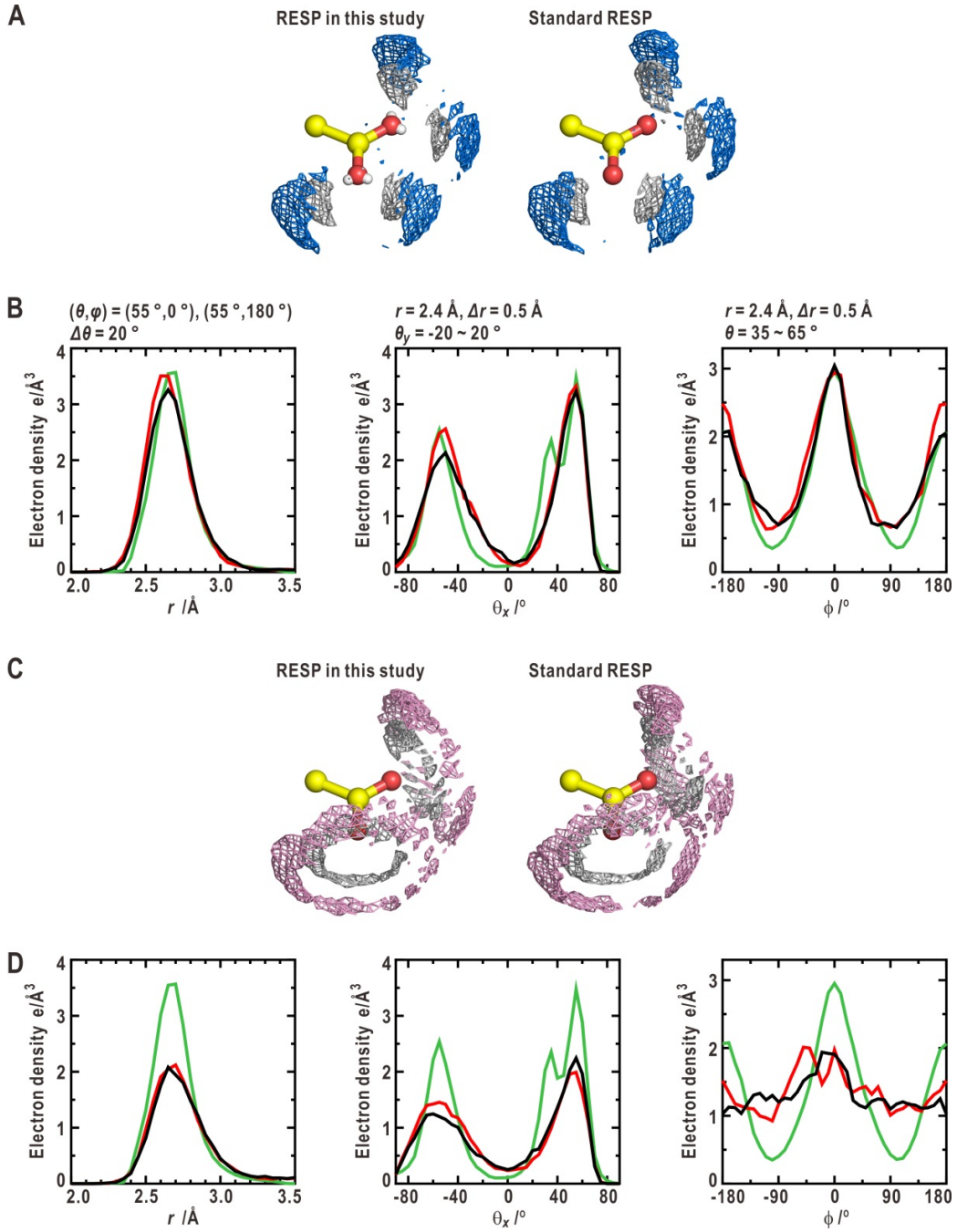

Supplementary Figure S12. (A) Solvent density maps around the OE1 and OE2 atoms in the side chain of glutamate in the GEKG peptide from the MD-LP simulations using the charges determined by the present (left) and the standard (right) RESP procedures. (B) Profiles of the distance (left),θ_x (center), and φ (right) distributions of oxygen atoms in hydration water molecules around the OE1 and OE2 atoms in

the EHDF (green line), the MD-LP simulations using the charges determined by the present (black) and the standard (red) RESP procedures. The distance distribution is calculated by averaging those in the four clusters of the solvent densities. In addition, the θ_x and φ distributions are averaged for the solvent densities around the OE1 and OE2 atoms. (C) Solvent density maps around the side chain of glutamate from the MD-noLP simulations using the charges determined by the present (left) and the standard (right) RESP procedures. (D) Profiles of the distance (left), θ_x (center), and φ (right) distributions of solvent densities around the OE1 and OE2 atoms in the MD-noLP simulations. The coloring scheme of the lines are the same with that in panel (B).

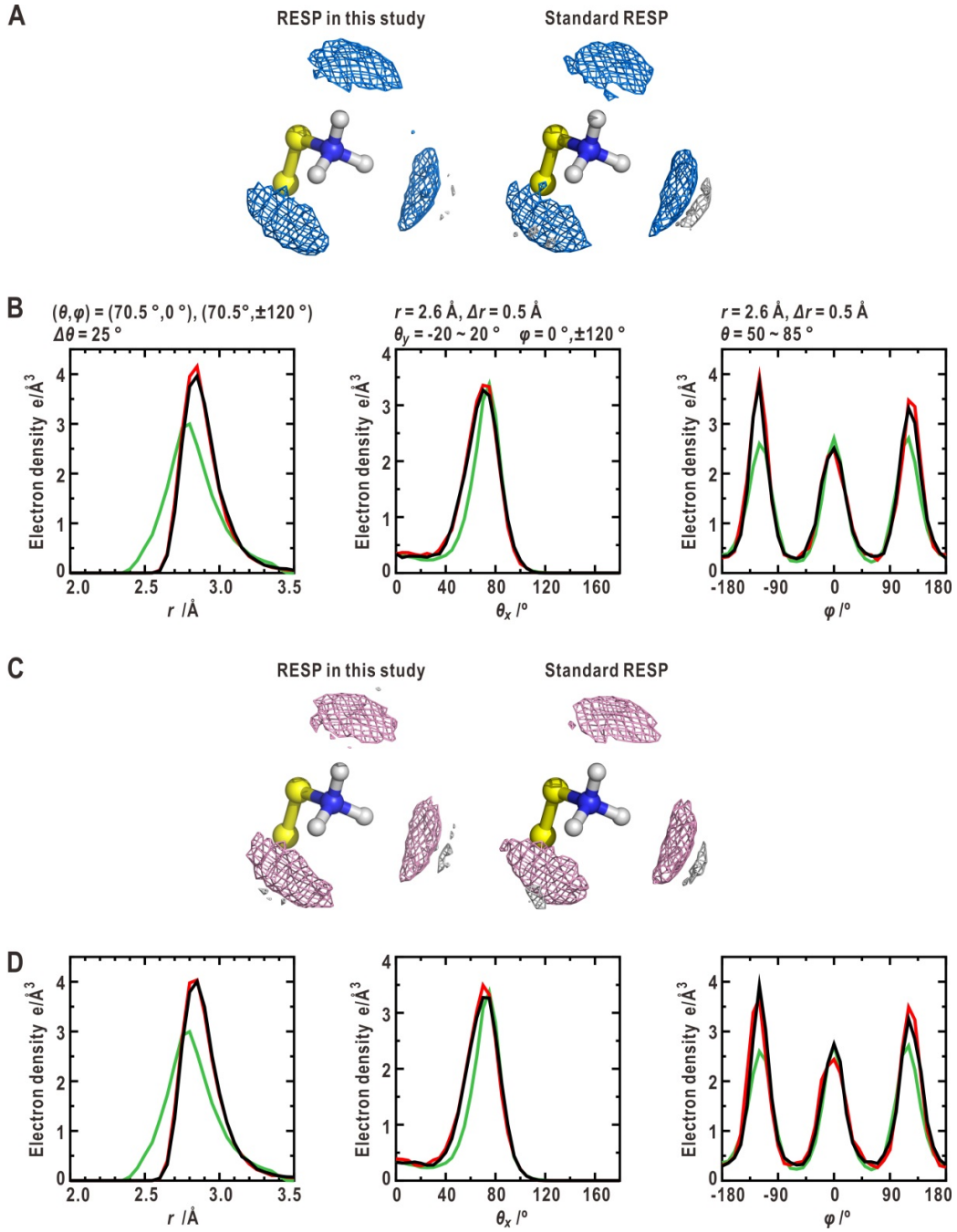

Supplementary Figure S13. (A) Solvent density maps around the NH_3^+ group in the side chain of lysine in the GEKG peptide from the MD-LP simulations using the charges determined by the present (left) and the standard (right) RESP procedures. (B) Profiles of distance (left panel), θ_x (center), and φ (right) distributions of oxygen atoms in hydration water molecules around the NH_3^+ group calculated

from the EHDF (green line), the MD-LP simulations using the charges determined by the present (black) and the standard (red) RESP procedures. The coordinate system used for calculating the profiles is shown in Figs 1B and 5A of the main text. (C) Solvent density maps from the MD-noLP simulations using the charges determined by the present (left) and the standard (right) RESP procedures. (D) Profiles of the distance (left panel), θ_x (center), and φ (right) distributions of the oxygen atoms in hydration water molecules around the NH_3^+ group in the MD-noLP simulations.

Supplementary Note 9: Influence of water models on the solvent density distribution in the MD-LP and MD-noLP simulations

The solvent densities in the EHDFs around the side chains of glutamate and lysine in the Gly-Glu-Lys-Gly peptide were compared among the MD-LP and MD-noLP simulations using the TIP3P[8] (Figure 1), TIP4P/Ew[9], TIP5P[10], and SPC/E[11] models (Supplementary Figs S14 and S15). While the solvent density distributions around the NH_3^+ group in the side chain of lysine were similar to the EHDF in all the simulations, those around the deprotonated oxygen atoms in the sp^2-hybridization in the side chain of glutamate depended on the models of water molecules as well as the two types of MD simulations.

In the MD-LP simulations using the TIP3P (Fig. 1), SPC/E (Supplementary Fig. S15A-B), and TIP4P/Ew (Supplementary Fig. S15C-D)) models, the distributions of oxygen atoms in hydration water molecules around the side chains of the glutamate residues resembled that of the EHDF with regard to the profiles and peak positions in the distance and angular distributions (Supplementary Table S5). Hydrogen atoms of hydration water molecules were localized along the OE1 (OE2)-LP directions between the OE1 (OE2) atom and the oxygen atoms of hydration water molecules. In the MD-LP simulations, the TIP3P model provided hydration structures that displayed the highest consistency with the EHDF among the three models.

In the MD-noLP simulations using the TIP3P (Fig. 1), SPC/E (Supplementary Fig. S15A-B), and TIP4P/Ew (Supplementary Fig. S15C-D) models, the distributions of oxygen atoms in hydration water molecules were inconsistent with those from the MD-LP simulations and in the EHDF. The solvent densities were distributed in toroidal shapes around the OE1 (OE2) atom at approximately $\theta = 55°$. In addition, the low density in the distance distribution suggested that the OE1 (OE2) atoms were less hydrated in the MD-noLP simulations than in the MD-LP simulations.

Both the MD-LP and MD-noLP simulations using the TIP5P model gave the distribution of the

oxygen atoms in hydration water molecules inconsistent with the EHDF (Supplementary Figs. S15E-F and Table S5). The solvent densities distributed in toroidal shapes around the OE1 (OE2) atoms resembled those from the MD-noLP simulations using the TIP3P, TIP4P/Ew, and SPC models rather than those from the MD-LP simulations using the three models (Supplementary Fig. S15F). The densities of the hydration water molecules in the toroidal shapes were significantly smaller than those in the MD-noLP simulations for the other models of water molecules.

Regarding the computational cost for MD simulations, the TIP4P/Ew model increases drastically the degrees of freedom of the simulation systems. In addition, the SPC/E model uses different configuration parameters to those obtained experimentally. For these reasons, the TIP3P model was selected as the model for water molecule in this simulation study.

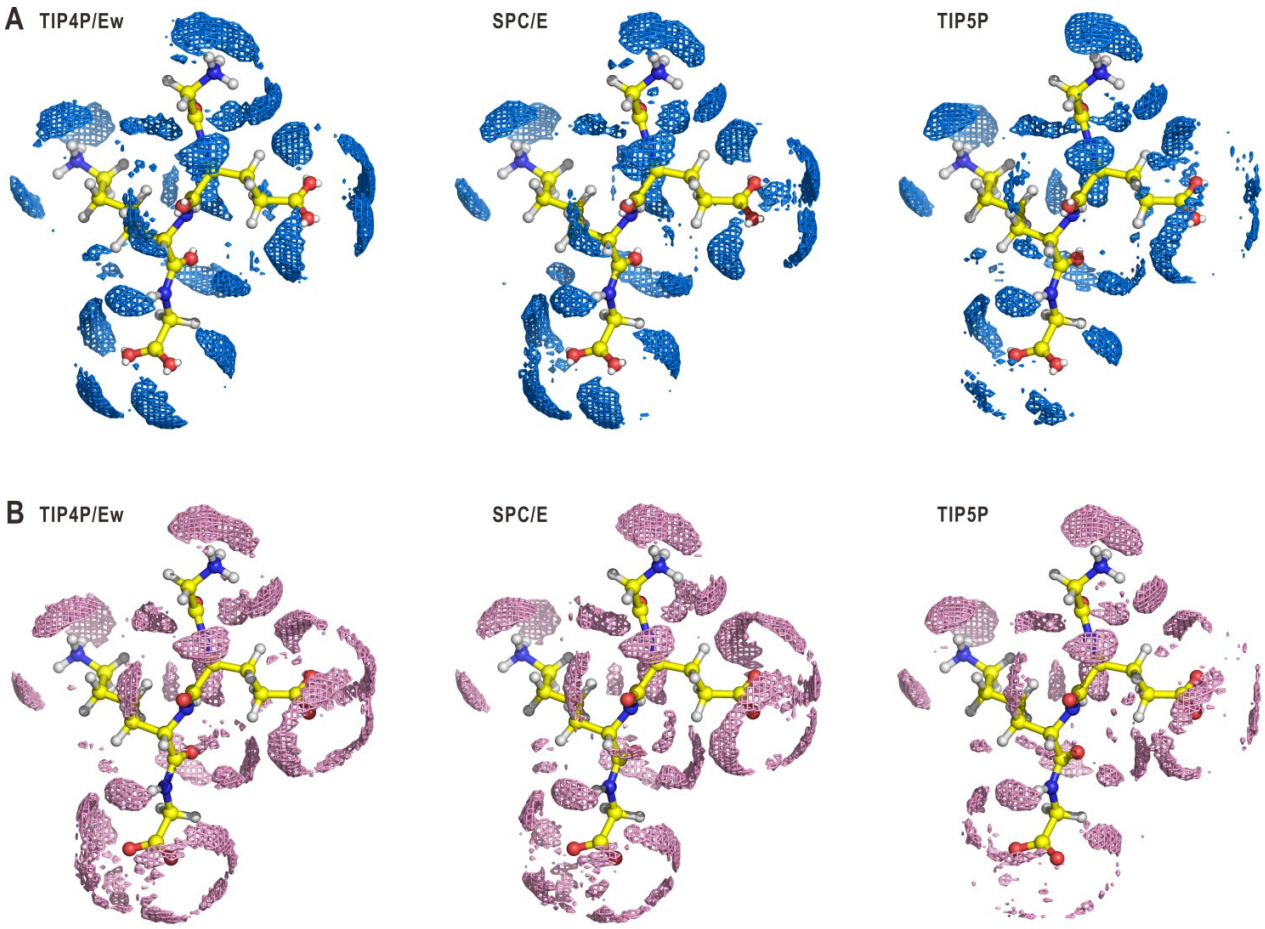

Supplementary Figure S14. Solvent density maps of water oxygen atoms from the MD-LP (A) and MD-noLP (B) simulations using the TIP4P/Ew, SPC/E, and TIP5P models.

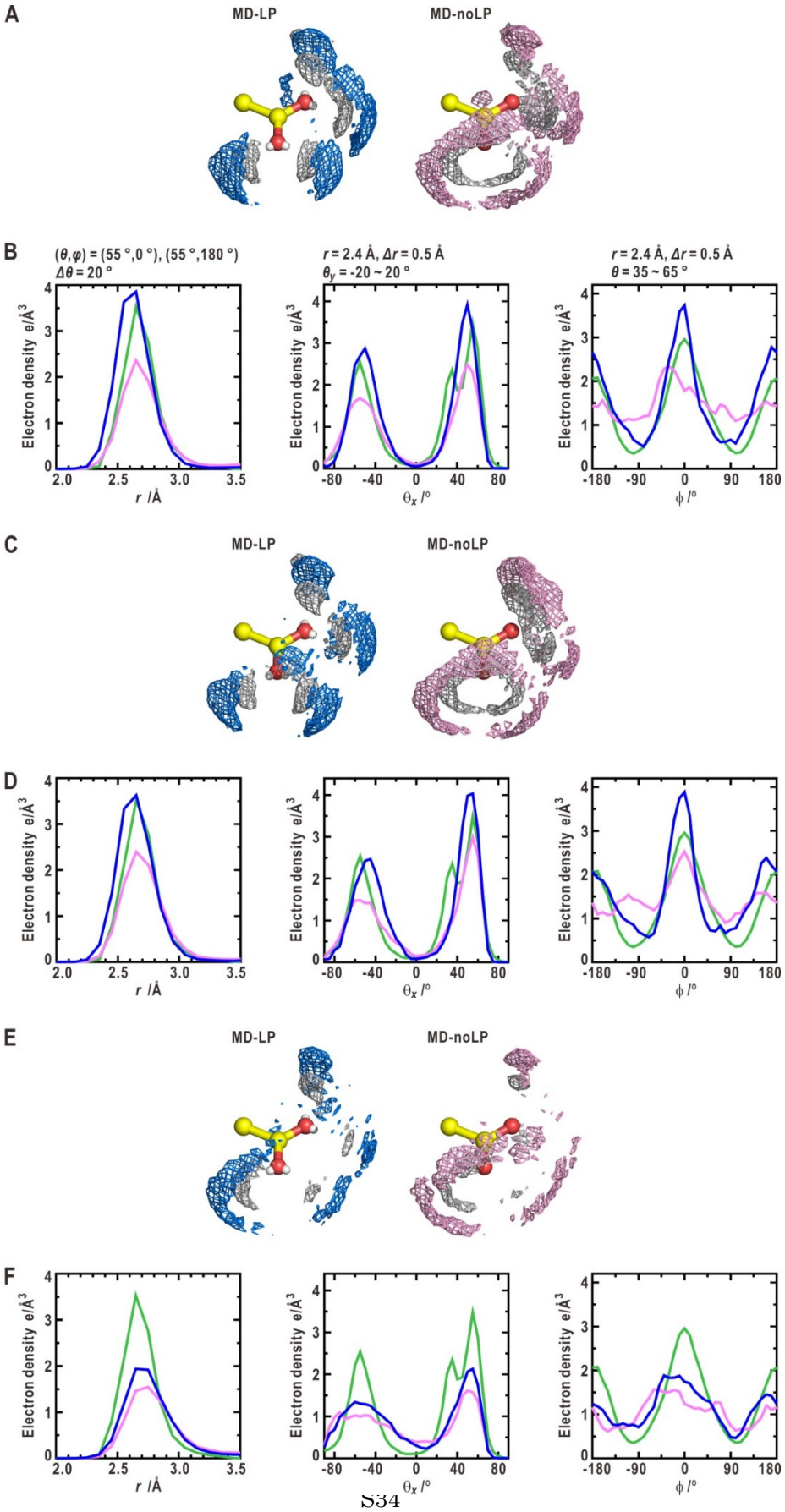
A
MD-LP
MD-noLP
B
(θ,φ) = (55 °,0 °), (55 °,180 °)
Δθ = 20 °
r = 2.4 Å, Δr = 0.5 Å
θy = -20 ~ 20 °
r = 2.4 Å, Δr = 0.5 Å
θ = 35 ~ 65 °
Electron density e/Å3
r /Å
θx /°
ϕ /°
C
MD-LP
MD-noLP
D
E
MD-LP
MD-noLP
F

Supplementary Figure S15. Solvent density maps around the OE1 and OE2 atoms in the side chain of glutamate in the GEKG peptide immersed in water bath composed of SPC/E (panels (A) and (B)), TIP4P/Ew ((C) and (D)), and TIP5P ((E) and (F)). Panels (A) illustrate solvent density maps of the MD-LP and MD-noLP simulations. Panels (C) and (E) compare the solvent density maps only from the MD-LP and MD-noLP simulations. Plots in panels (B), (D) and (F) are profiles of the distance (left), θ_x (center), and φ (right) distributions, respectively. The distributions are averaged for the OE1 and OE2 atoms.

Supplementary Table S1. Atom-centered and off-atom charges of amino acids determined by the RESP protocol applied to the non-blocked tri- and tetrapeptides. In this study, even though the hydration structures calculated from the MD simulations are not shown for glutamine and asparagine owing to the reasons described in the Methods section in the main text, it is possible to perform calculations for these amino acids. The determined charges are also listed in this table.

Without LP electrons		**With LP electrons**	
Charge site	**Charges**	**Charge site**	**Charges**
		Glutamate	
N	-0.860084	N	-0.897270
H	0.412786	H	0.444355
CA	0.092112	CA	0.110056
HA	0.121019	HA	0.133800
CB	-0.035896	CB	-0.067795
HB2	0.054904	HB2	0.059574
HB3	0.054904	HB3	0.059574
CG	-0.218415	CG	-0.032361
HG2	0.037065	HG2	0.027754
HG3	0.037065	HG3	0.027754
CD	0.853802	CD	0.282909
OE1	-0.812340	OE1	0.147905
		EP+2	-0.369598
		EP-2	-0.369598
OE2	-0.812340	OE2	0.147905
		EP+3	-0.369598
		EP-3	-0.369598
C	0.692408	C	0.539877
O	-0.616991	O	0.017428
		EP+1	-0.261537
		EP-1	-0.261537
		Aspartate	
N	-0.756298	N	-0.763484

H	0.328416	H	0.354540
CA	0.113297	CA	0.115410
HA	0.160166	HA	0.169097
CB	-0.167596	CB	0.010446
HB2	0.024299	HB2	0.024862
HB3	0.024299	HB3	0.024862
CG	0.946202	CG	0.254448
OD1	-0.834253	OD1	0.321168
		EP+2	-0.442113
		EP-2	-0.442113
OD2	-0.834253	OD2	0.321168
		EP+3	-0.442113
		EP-3	-0.442113
C	0.560599	C	0.378814
O	-0.564879	O	0.051607
		EP+1	-0.247243
		EP-1	-0.247243
	Glutamine		
N	-0.682793	N	-0.755351
H	0.350114	H	0.387719
CA	-0.022417	CA	0.030970
HA	0.121897	HA	0.121812
CB	-0.029233	CB	-0.034917
HB2	0.063041	HB2	0.060355
HB3	0.063041	HB3	0.060355
CG	-0.150655	CG	-0.089306
HG2	0.044707	HG2	0.046883
HG3	0.044707	HG3	0.046883
CD	0.824478	CD	0.528456
OE1	-0.670600	OE1	-0.002312
		EP+2	-0.260920
		EP-2	-0.260920
NE2	-0.998395	NE2	-0.842063
HE21	0.440747	HE21	0.407452
HE22	0.440747	HE22	0.407452

C	0.677120	C	0.566932
O	-0.516505	O	-0.025418
		EP+1	-0.197031
		EP-1	-0.197031
Asparagine			
N	-0.818266	N	-0.847976
H	0.431191	H	0.451542
CA	0.015689	CA	0.006041
HA	0.149543	HA	0.164574
CB	-0.283303	CB	-0.128210
HB2	0.100889	HB2	0.079323
HB3	0.100889	HB3	0.079323
CG	1.020677	CG	0.668810
OD1	-0.678941	OD1	0.007457
		EP+2	-0.265544
		EP-2	-0.265544
ND2	-1.198126	ND2	-0.986155
HD21	0.480515	HD21	0.428524
HD22	0.480515	HD22	0.428524
C	0.742199	C	0.627923
O	-0.543472	O	0.001741
		EP+1	-0.225177
		EP-1	-0.225177
Histidine (HIE state)			
N	-0.707833	N	-0.673708
H	0.350429	H	0.341525
CA	-0.118901	CA	-0.143296
HA	0.119894	HA	0.147683
CB	0.209102	CB	-0.036344
HB2	0.057808	HB2	0.123191
HB3	0.057808	HB3	0.123191
CG	0.043331	CG	0.000511
ND1	-0.602935	ND1	0.750273
		EP21	-0.985622
CE1	0.208554	CE1	0. 032377

HE1	0.177379	HE1	0. 195482
NE2	-0.382473	NE2	-0.462307
HE2	0.323602	HE2	0.383779
CD2	0.063033	CD2	-0.102355
HD2	0.041454	HD2	0.114394
C	0.760819	C	0.730600
O	-0.601071	O	-0.014726
		EP+1	-0.262324
		EP-1	-0.262324
Histidine (HID state)			
N	-0.767585	N	-0.804036
H	0.394737	H	0.422881
CA	-0.058966	CA	-0.016400
HA	0.136588	HA	0.127834
CB	-0.108693	CB	-0.047121
HB2	0.094819	HB2	0.092793
HB3	0.094819	HB3	0.092793
CG	0.043331	CG	-0.026425
ND1	-0.305373	ND1	-0.469971
HD1	0.338677	HD1	0.419451
CE1	0.208554	CE1	0.044763
HE1	0.131981	HE1	0.171860
NE2	-0.602935	NE2	0.797775
		EP21	-1.033835
CD2	0.063033	CD2	-0.114868
HD2	0.134017	HD2	0.167909
C	0.825673	C	0.701662
O	-0.622677	O	-0.001193
		EP+1	-0.262936
		EP-1	-0.262936
Tyrosine (sp^2)			
N	-0.761937	N	-0.805355
H	0.389733	H	0.420181
CA	-0.034787	CA	0.019751
HA	0.134237	HA	0.115700

CB	-0.04492	CB	-0.032844
HB2	0.070234	HB2	0.062867
HB3	0.070234	HB3	0.062867
CG	0.02709	CG	0.0334767
CD1	-0.172006	CD1	-0.165339
HD1	0.150039	HD1	0.141810
CE1	-0.202585	CE1	-0.148310
HE1	0.157342	HE1	0.149371
CZ	0.246838	CZ	0. 031089
OH	-0.54875	OH	-0.016274
		EP21	-0.326425
HH	0.412294	HH	0.326884
CE2	-0.202585	CE2	-0.148310
HE2	0.157342	HE2	0.149371
CD2	-0.172006	CD2	-0.165339
HD2	0.150039	HD2	0.141810
C	0.788008	C	0.676862
O	-0.613854	O	0.000084
		EP+1	-0.262610
		EP-1	-0.262610
Tyrosine (sp^3)			
		N	-0.802499
		H	0.418274
		CA	0.019196
		HA	0.115350
		CB	-0.024854
		HB2	0.061479
		HB3	0.061479
		CG	0.033283
		CD1	-0.175104
		HD1	0.148891
		CE1	-0.178668
		HE1	0.153794
		CZ	0.132394
		OH	-0.018206

		EP+2	-0.194325
		EP-2	-0.194325
		HH	0.344061
		CE2	-0.178668
		HE2	0.153794
		CD2	-0.175104
		HD2	0.148891
		C	0.675891
		O	0.000788
		EP+1	-0.262907
		EP-1	-0.262907
Serine			
N	-0.708549	N	-0.752784
H	0.381975	H	0.409710
CA	0.020266	CA	0.084222
HA	0.192246	HA	0.171601
CB	0.072273	CB	0.032613
HB2	0.075861	HB2	0.060899
HB3	0.075861	HB3	0.060899
OG	-0.649230	OG	-0.024236
HG	0.440238	HG	0.361709
		EP+2	-0.244436
		EP-2	-0.244436
C	0.691544	C	0.598567
O	-0.592484	O	0.001621
		EP+1	-0.257975
		EP-1	-0.257975
Threonine			
N	-0.760940	N	-0.837103
H	0.397030	H	0.421759
CA	0.123464	CA	0.304277
HA	0.175883	HA	0.118985
CB	0.136428	CB	0.089172
HB	0.054611	HB	0.033819
CG2	-0.14856	CG2	-0.111582

HG21	0.058564	HG21	0.043062
HG22	0.058564	HG22	0.043062
HG23	0.058564	HG23	0.043062
OG1	-0.666196	OG1	-0.041629
HG1	0.428784	HG1	0.349871
		EP+2	-0.247979
		EP-2	-0.247979
C	0.675438	C	0.548043
O	-0.591634	O	-0.008613
		EP+1	-0.250113
		EP-1	-0.250113
		Lysine	
N	-0.470293	N	-0.488756
H	0.250043	H	0.258437
CA	-0.041329	CA	0.008918
HA	0.107966	HA	0.099785
CB	-0.017259	CB	-0.010584
HB2	0.011460	HB2	0.009803
HB3	0.011460	HB3	0.009803
CG	-0.015464	CG	-0.019098
HG2	0.005667	HG2	0.013106
HG3	0.005667	HG3	0.013106
CD	0.009944	CD	-0.001239
HD2	0.036693	HD2	0.037163
HD3	0.036693	HD3	0.037163
CE	0.067301	CE	0.060503
HE2	0.108924	HE2	0.106623
HE3	0.108924	HE3	0.106623
NZ	-0.660955	NZ	-0.597710
HZ1	0.405830	HZ1	0.389236
HZ2	0.405830	HZ2	0.389236
HZ3	0.405830	HZ3	0.389236
C	0.877101	C	0.759068
O	-0.650029	O	-0.016678
		EP+1	-0.276873

		EP-1	-0.276873
Arginine			
N	-0.451629	N	-0.489554
H	0.260148	H	0.264567
CA	-0.060903	CA	-0.017389
HA	0.104496	HA	0.107680
CB	-0.021906	CB	-0.009199
HB2	0.017296	HB2	0.015842
HB3	0.017296	HB3	0.015842
CG	0.031084	CG	0.020851
HG2	0.005058	HG2	0.014496
HG3	0.005058	HG3	0.014496
CD	0.029314	CD	-0.004762
HD2	0.095248	HD2	0.105133
HD3	0.095248	HD3	0.105133
NE	-0.569153	NE	-0.550419
HE	0.389115	HE	0.387120
CZ	0.793842	CZ	0.775401
NH1	-0.875346	NH1	-0.866861
HH11	0.447645	HH11	0.445699
HH12	0.447645	HH12	0.445699
NH2	-0.875346	NH2	-0.866861
HH21	0.447645	HH21	0.445699
HH22	0.447645	HH22	0.445699
C	0.860863	C	0.735457
O	-0.640365	O	-0.029726
		EP+1	-0.255022
		EP-1	-0.255022
Tryptophan			
N	-0.775714	N	-0.791969
H	0.396418	H	0.414489
CA	-0.016596	CA	0.027656
HA	0.144761	HA	0.132769
CB	-0.101428	CB	-0.066863
HB2	0.101584	HB2	0.093188

HB3	0.101584	HB3	0.093188
CG	-0.076610	CG	-0.098367
CD1	-0.081668	CD1	-0.057900
HD1	0.125415	HD1	0.104909
NE1	-0.459363	NE1	-0.457924
HE1	0.386072	HE1	0.385290
CE2	0.115048	CE2	0.110693
CZ2	-0.163021	CZ2	-0.159764
HZ2	0.130626	HZ2	0.129805
CH2	-0.157693	CH2	-0.158941
HH2	0.149862	HH2	0.149856
CZ3	-0.203775	CZ3	-0.203544
HZ3	0.151567	HZ3	0.151606
CE3	-0.129678	CE3	-0.124226
HE3	0.142544	HE3	0.139374
CD2	0.048724	CD2	0.046696
C	0.791474	C	0.669067
O	-0.620131	O	-0.006476
		EP+1	-0.261305
		EP-1	-0.261305

Supplementary Table S2. The number of possible hydrogen bonds formed between the polar atoms of the hydrophilic amino acids and hydration water molecules.

Amino acid	Atom	Hybridization	Number of lone pairs/bonds with H	Number of possible hydrogen bonds
Peptide bond	O	sp^2	2/0	2
	N	sp^2	0/1	1
Glu	OE1	sp^2	2/0	2
	OE2	sp^2	2/0	2
Asn	OD1	sp^2	2/0	2
	OD2	sp^2	2/0	2
Gln	OE1	sp^2	2/0	2
	NE2	sp^2	0/2	2
Asn	OD1	sp^2	2/0	2
	ND2	sp^2	0/2	2
His (HIE)	ND1	sp^2	1/0	1
	NE2	sp^2	0/1	1
His (HID)	ND1	sp^2	0/1	1
	NE2	sp^2	1/0	1
Tyr	OH	sp^2	1/1	2
	OH	sp^3	2/1	3
Ser	OG	sp^3	2/1	3
Thr	OG1	sp^3	2/1	3
Lys	NZ	sp^3	0/3	3
Arg	NE	sp^2	0/1	1
	NH1	sp^2	0/2	2
	NH2	sp^2	0/2	2
Trp	NE1	sp^2	0/1	1

Supplementary Table S3. The relative root-mean-square (RRMS) errors of ESP that are calculated from the charges determined by the RESP procedure using the restraint strength of 0.001 au. The values in brackets are the RRMS errors when using the restraint strength of 0.0005 au.

Peptide	RRMS[a] (without LP electrons)	RRMS[a] (with LP electrons)
GEKG	0.0224 (0.0220)	0.0236 (0.0225)
GERG	0.0224 (0.0217)	0.0235 (0.0223)
GDKG	0.0338 (0.0329)	0.0306 (0.0298)
GQG	0.0272 (0.0266)	0.0285 (0.0274)
GNG	0.0269 (0.0262)	0.0284 (0.0273)
GHG (HIE state)	0.0362 (0.0353)	0.0327 (0.0316)
GHG (HID state)	0.0296 (0.0286)	0.0336 (0.0331)
GYG (sp^2)	0.0280 (0.268)	0.0290 (0.0278)
GYG (sp^3)		0.0307 (0.0299)
GSG	0.0257 (0.0252)	0.0260 (0.0254)
GTG	0.0277 (0.0264)	0.0288 (0.0274)
GWG	0.0270 (0.0261)	0.0273 (0.0263)

[a] $RRMS = \left(\sum_{i=1}^{N_{\mathrm{ESP}}} \left(\hat{V}_i - V_i \right)^2 \Big/ \sum_{i=1}^{N_{\mathrm{ESP}}} V_i^2 \right)^{1/2}$, where N_{ESP}, V_i, and $\hat{V}_i$ refer to the number of ESP points, the QM ESP, and ESP calculated from the charges determined by the RESP procedure, respectively.

Supplementary Table S4. Atom-centered and off-atom charges of amino acids determined by the standard RESP protocol applied to the blocked di-peptides.

Without LP electrons		With LP electrons	
Charge site	**Charges**	**Charge site**	**Charges**
		Glutamate	
N	-0.489110	N	-0.519193
H	0.255155	H	0.278576
CA	0.070501	CA	0.064514
HA	0.120070	HA	0.132664
CB	0.015423	CB	0.015664
HB2	0.004160	HB2	0.010070
HB3	0.004160	HB3	0.010070
CG	-0.018505	CG	0.033277
HG2	-0.024488	HG2	-0.011041
HG3	-0.024488	HG3	-0.011041
CD	0.795881	CD	0.279730
OE1	-0.819333	OE1	0.219928
		EP+2	-0.411414
		EP-2	-0.411414
OE2	-0.819333	OE2	0.219928
		EP+3	-0.411414
		EP-3	-0.411414
C	0.431213	C	0.334958
O	-0.501305	O	0.025703
		EP+1	-0.219075
		EP-1	-0.219075
		Lysine	
N	-0. 346760	N	-0.377489
H	0. 225628	H	0.251560
CA	0.013229	CA	0.011366
HA	0.068248	HA	0.074435
CB	-0.025609	CB	-0.019488
HB2	0.022544	HB2	0.021336

HB3	0.022544	HB3	0.021336
CG	0.012107	CG	0.010336
HG2	0.013167	HG2	0.013399
HG3	0.013167	HG3	0.013399
CD	-0.023662	CD	-0.022498
HD2	0.060025	HD2	0.059861
HD3	0.060025	HD3	0.059861
CE	0.019098	CE	0.019392
HE2	0.110639	HE2	0.110867
HE3	0.110639	HE3	0.110867
NZ	-0.584280	NZ	-0.592338
HZ1	0.393432	HZ1	0.395896
HZ2	0.393432	HZ2	0.395896
HZ3	0.393432	HZ3	0.395896
C	0.564585	C	0.479401
O	-0.515633	O	0.016723
		EP+1	-0.225007
		EP-1	-0.225007

Supplementary Table S5. The positions of the peaks in the density distributions.

Amino acid	Distribution type	Peak positions in MD-LP	Peak positions in MD-noLP
Glu (TIP4P/Ew)	r /Å	2.65 (0.15)	2.65 (0.17)
	θ_x /°	-50 (15), 50 (12)	-55 (19), 50 (13)
	φ /°	0 (29), 170 (34)	-30 (30)
	Total amount of water densities around COO^- group [b]	4.6	4.5
Glu (SPC/E)	r /Å	2.65 (0.16)	2.65 (0.17)
	θ_x /°	-45 (17), 55 (11)	-55 (19), 55 (11)
	φ /°	-5 (25), 165 (33),	0 (25)
	Total amount of water densities around COO^- group [b]	4.6	4.6
Glu (TIP5P)	r /Å	2.65 (0.18)	2.75 (0.20)
	θ_x /°	-60 (32), 55 (14)	-60 (53), 50 (14)
	φ /°	-10 (68), 160 (36)	None
	Total amount of water densities around COO^- group [b]	4.1	3.8

References

1. Dixon, R. W. & Kollman, P. A. Advancing beyond the atom-centered model in additive and nonadditive molecular mechanics. *J. Comput. Chem.* **18**, 1632-1646 (1997).
2. Lu, Z., Zhou, N., Wu, Q. & Zhang, Y. Directional dependence of hydrogen bonds: a density-based energy decomposition analysis and its implications on force field development. *J. Chem. Theory Comput.* **7**, 4038–4049 (2011).
3. Baker, E. N.; Hubbard, R. E. Hydrogen bonding in globular proteins. *Prog. Biophys. Mol. Biol.* **44**, 97-179 (1984).
4. Ippolito, J. A., Alexander, R. S. & Christianson, D. W. Hydrogen bond stereochemistry in protein structure and function. *J. Mol. Biol.* **215**, 457-471 (1990).
5. Matsuoka, D. & Nakasako, M. Probability distributions of hydration water molecules around polar protein atoms obtained by a database analysis. *J. Phys. Chem. B* **113**, 11274-11292 (2009).
6. Cornell, W. D. *et al.* A second generation force field for the simulation of proteins, nucleic acids, and organic molecules. *J. Am. Chem. Soc.* **117**, 5179-5197 (1995).
7. Cieplak, P., Cornell, W. D., Bayly, C. & Kollman P. A. Application of the multimolecule and multiconfomational RESP methodology to biopolymers: charge derivation for DNA, RNA, and proteins. *J. Chem. Comput.* **16***,* 1357-1377 (1995).
8. Jorgensen, W. L., Chandrasekhar, J., Madura, J. D., Impey, R. W. & Klein, M. L. Comparison of simple potential functions for simulating liquid water. *J. Chem. Phys.* **79**, 926-935 (1983).
9. Horn, H. W. *et al.* Development of an improved four-site water model for biomolecular simulations. *J. Chem. Phys.* **120**, 9665-9678 (2004).
10. Mahoney, M. W. & Jorgensen, W. L. A five-site model for liquid water and the reproduction of the density anomaly by rigid, nonpolarizable potential functions. *J. Chem. Phys.* **112**, 8910-8922 (2000).

11. Berendsen, H. J. C., Grigera, J. R. & Straatsma, T. P. The missing term in effective pair potentials. *J. Phys. Chem.* **91**, 6269-6271 (1987).